© 2019. Published by The Company of Biologists Ltd | Journal of Experimental Biology (2019) 222, jeb198085. doi:10.1242/jeb.198085

RESEARCH ARTICLE

Context-dependent scaling of kinematics and energetics during contests and feeding in mantis shrimp

P. A. Green[1,*], M. J. McHenry[2] and S. N. Patek[1]

ABSTRACT

Measurements of energy use, and its scaling with size, are critical to understanding how organisms accomplish myriad tasks. For example, energy budgets are central to game theory models of assessment during contests and underlie patterns of feeding behavior. Clear tests connecting energy to behavioral theory require measurements of the energy use of single individuals for particular behaviors. Many species of mantis shrimp (Stomatopoda: Crustacea) use elastic energy storage to power high-speed strikes that they deliver to opponents during territorial contests and to hard–shelled prey while feeding. We compared the scaling of strike kinematics and energetics between feeding and contests in the mantis shrimp *Neogonodactylus bredini*. We filmed strikes with high-speed video, measured strike velocity and used a mathematical model to calculate strike energy. During contests, strike velocity did not scale with body size but strike energy scaled positively with size. Conversely, while feeding, strike velocity decreased with increasing size and strike energy did not vary according to body size. Individuals most likely achieved this strike variation through differential compression of their exoskeletal spring prior to the strike. *Post hoc* analyses found that *N. bredini* used greater velocity and energy when striking larger opponents, yet variation in prey size was not accompanied by varying strike velocity or energetics. Our estimates of energetics inform prior tests of contest and feeding behavior in this species. More broadly, our findings elucidate the role behavioral context plays in measurements of animal performance.

KEY WORDS: Velocity, Energy, Scaling, Animal weapons, Animal contests, Stomatopod

INTRODUCTION

Energy is a central currency in biology that fuels how animals accomplish essential tasks. Therefore, theoretical models describing diverse animal behaviors often hinge on how animals use energy. For example, game theory models of contest assessment behavior assume that energy budgets dictate competitive persistence (Briffa and Sneddon, 2007; Payne, 1988), and animal foraging behavior is theorized to be determined, at least in part, by the energy used to find and process prey (Pyke, 1984).

Experimental tests of how animals use energy in specific behavioral contexts have been important in validating and informing behavioral theory. Techniques such as labeled water measurements and time budget observations (e.g. Utter and LeFebvre, 1973; Weathers and Nagy, 1980) have revealed how animals parse out limited energetic stores across behavioral tasks. For example, Vehrencamp et al. (1989) measured energy use by injecting and later resampling doubly labeled water from courting male sage grouse. They found that energy use scaled positively with courtship effort, but behavioral observations showed that males courting most frequently afforded these costs by foraging more than other males (Vehrencamp et al., 1989). More recently, advances in measuring metabolic proxies such as oxygen consumption (or carbon dioxide production), as well as tools such as heart rate telemetry, have enabled finer-resolution measurements of the energetic costs of individual behaviors. Barske et al. (2014) measured the heart rates of male golden-collared manakins as they performed jump–snap displays toward females and inferred energy use from laboratory-based calibrations of oxygen metabolism against heart rate. They found that displays required only ∼1% of a male's daily energy expenditure, countering predictions of sexual selection theory that male displays involve high energetic costs (Barske et al., 2014). These and other studies of energy use in behavioral contexts (e.g. Boisseau et al., 2017; DeCarvalho et al., 2004; Hack, 1997; Reichert, 1988) have lent insight into theory, and recent reviews have called for more measurements of energy use in contexts such as courtship (Byers et al., 2010; Clark, 2012) and competition (Briffa and Sneddon, 2007). However, direct tests of context- and behavior-specific energetics remain few.

Direct energetic measurements of single individuals performing single behaviors, in or across specific contexts, are difficult. Techniques such as oxygen metabolism measurements allow researchers to directly quantify the energetics of specific behaviors; however, because some contexts (e.g. courtship, competition) involve two or more interacting individuals, it can be hard to isolate measurements to a single individual. For example, DeCarvalho et al. (2004) used oxygen metabolism measurements to show that escalating contest behaviors (e.g. grappling versus displaying) in dueling sierra dome spiders resulted in higher energetic costs, matching game-theory models. However, these researchers were unable to isolate each competing individual from a given dyad; instead, they halved a combined oxygen consumption rate to infer an individual's energy use (DeCarvalho et al., 2004). Although other measures such as lactate production can allow for energy measurements of a single individual, these must be measured at the end of an interaction (e.g. Briffa and Elwood, 2001) and therefore cannot quantify the cost of single behaviors. To better understand how energy is used by single individuals, for single behaviors, in or across specific contexts, novel study systems and techniques are required.

Mantis shrimp (Stomatopoda: Crustacea) offer a tractable system for measuring individual-level, behavior-specific energetics, both across behavioral contexts and along a continuum of body size. Smashing mantis shrimp, such as the Caribbean species *Neogonodactylus bredini*, use their spring-powered raptorial

[1]Biology Department, Duke University, Durham, NC 27708, USA. [2]Department of Ecology and Evolutionary Biology, University of California, Irvine, Irvine, CA 92697, USA.

*Author for correspondence (pag16@duke.edu)

P.A.G., 0000-0002-2434-8795; S.N.P., 0000-0001-9738-882X

Received 13 December 2018; Accepted 13 March 2019

Journal of Experimental Biology (2019) 222, jeb198085. doi:10.1242/jeb.198085

List of symbols and abbreviations

I	moment of inertia (kg m^2), measured for both the striking body and the added mass of water
AIC	Akaike information criterion
E_{spring}	elastic potential energy of the spring system (J)
E_{KE}	strike kinetic energy (J)
E_{drag}	energy lost to drag (J)
E_{strike}	total strike energy (J)
k	torsion spring stiffness (N m rad^{-1})
LMM	linear mixed model
RMR	resting metabolic rate
γ	angular position (rad)
$\Delta\theta$	spring rotation, relative to resting position (deg)
τ	torque generated by drag (N m)
ω	angular velocity (rad s^{-1})
ω_{max}	maximum angular velocity (rad s^{-1})

appendages to deliver high-force strikes in two distinct contexts: contests and feeding (Fig. 1). During contests over burrows in coral rubble, *N. bredini* ritualistically exchange strikes on their opponent's armored tailplate (Caldwell, 1987; Caldwell and Dingle, 1975; Dingle and Caldwell, 1969) in a behavior termed 'telson sparring' (Green and Patek, 2015). Telson sparring functions in mutual assessment of competitor body mass (Green and Patek, 2018) and, in body-length-matched contests, winners deliver a greater number of strikes than losers (Green and Patek, 2015). *Neogonodactylus bredini* also use strikes to feed on hard-shelled prey, which make up a substantial portion of their diet (deVries et al., 2016). Indeed, *N. bredini* are considered voracious snail predators (Caldwell et al., 1989). While feeding, *N. bredini* deliver an average of over 70 strikes, strategically moving from the aperture of the shell to the apex and maximizing shell damage (Crane et al., 2018). Because the strikes delivered to competitors and prey use the same appendage and the same motion (Fig. 1), measurements of strike energetics can be compared between these contexts.

Analyses of the energetic costs of mantis shrimp strikes have been enabled by a history of biomechanical study and advances in high-speed imaging and mathematical modeling. In preparation for a strike, extensor muscles in the merus segment contract and compress an exoskeletal elastic mechanism (the spring). Simultaneously, merus flexor muscles engage latches (modified apodemes) that prevent distal rotation of the striking body (defined as the combined propodus and dactyl segments that serve as a hammer) while the spring is loaded. Upon latch release, the spring's elastic potential energy transitions to kinetic energy, such that work is performed to rotate the striking body toward its target and to resist drag forces (for detailed descriptions of the strike mechanism, see Burrows, 1969; Burrows and Hoyle, 1972; Cox et al., 2014; McHenry et al., 2012, 2016; McNeill et al., 1972; Patek et al., 2004, 2007, 2013; Rosario and Patek, 2015; Zack et al., 2009). Strike duration is so short that smashing mantis shrimp must use open loop control: in order to vary kinematic output, they adjust elastic energy storage prior to striking by compressing the spring to different displacements (Kagaya and Patek, 2016). Increased extensor muscle activity causes greater shortening of the compression spring, thereby storing more elastic energy and resulting in a higher angular velocity of the strike (Kagaya and Patek, 2016). These studies, along with the development of a vetted mathematical model of strike energetics (McHenry et al., 2016, 2012), allow for measurements of strike kinematics to be connected with two types of energy: elastic energy storage (input) and combined strike kinetic and drag energy (output).

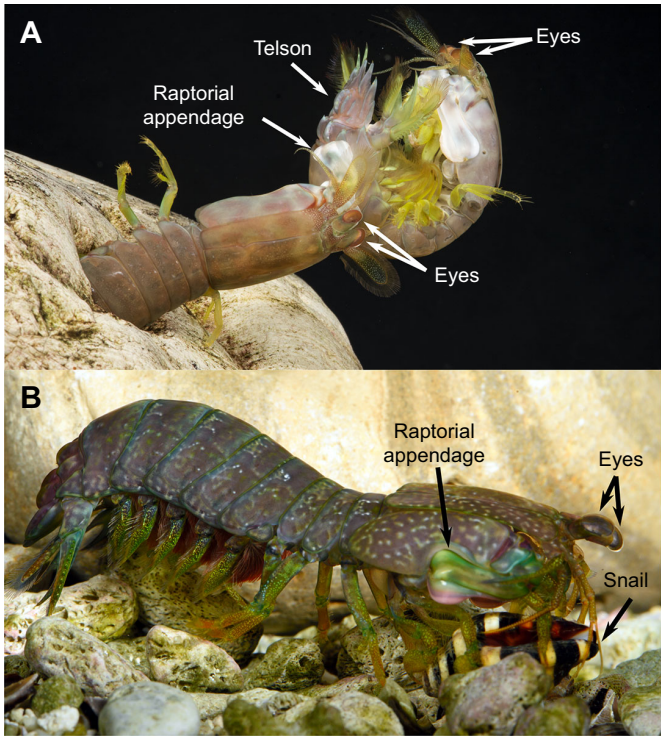

Fig. 1. Mantis shrimp use raptorial appendages to strike competitors and prey. (A) When mantis shrimp fight, they perform telson sparring. In this image, the individual on the left is rotated sideways (dorsal out of page), striking the opponent's telson with its left raptorial appendage. The individual on the right has its telson coiled in front of its body in a defensive posture. Both animals are *Neogonodactylus wennerae*, closely related to *N. bredini* (the focus of the present study). (B) Mantis shrimp use these same appendages for feeding. Here, *N. bredini* is preparing to strike a snail, with its appendage loaded in a pre-strike position (dorsal to top of image). Photo credits: Roy Caldwell.

Here, we measured how strike kinematics and energetics scale across body size, during feeding and contests, in *N. bredini*. Our goal was to measure the energetics of each strike for a given individual, rather than energetics of the whole organism. We measured maximum angular velocity using high-speed imaging during both behavioral contexts. We then applied a mathematical model to calculate energetics from these experimentally determined kinematics. We also used the mathematical model to simulate the amount of exoskeletal spring compression required to generate strike energetics. We addressed the following three questions. (1) Does the scaling of strike kinematics and energetics differ between behavioral contexts? Research on sparring strikes used for body mass signaling (Green and Patek, 2018) and feeding strikes used for opening durable prey (Crane et al., 2018; deVries et al., 2016; Full et al., 1989) have left unresolved how kinematics and energetics scale with body mass within a behavioral context or between contexts. (2) How do strike energetics relate to the required compression of the exoskeletal spring? Given that spring compression is positively correlated with strike velocity (Kagaya and Patek, 2016), we predict that, regardless of behavioral context, strike energy is positively correlated with spring compression. (3) Do individuals alter strike kinematics and energetics depending on the relative size of opponents or prey? Given the function of sparring strikes in mutual assessment (Green and Patek, 2018) and of feeding strikes in strategic prey processing (Crane et al., 2018), we predict that mantis shrimp adjust kinematics and energetics according to opponent and prey size.

MATERIALS AND METHODS

Experimental measurements

Animal collection and care

We collected male and female *Neogonodactylus bredini* (Manning 1969) from burrows in coral rubble in *Thalassia* spp. seagrass habitats on the Atlantic coast of Panama [Autoridad Nacional del Ambiente (ANAM) collection permits SE/A-115-13; SE/A-92-15; SE/A-52-17]. All individuals had a body length greater than 28 mm. *Neogonodactylus bredini* larger than approximately 30 mm body length are considered adults that compete for burrows and strike snails (deVries et al., 2016; Dingle, 1969); all individuals used in this study readily struck both competitors and prey items. We used a total of 13 individuals in this study; most were used in field-based studies of contest behavior (Green and Patek, 2015, 2018) before being transported to Duke University (ANAM export permits SEX/A-23-14; SEX/A-106-15; SEX/A-48-17). At Duke, they were housed individually in clear plastic cubes (10×10×10 cm, AMAC Plastics Corp., Sausalito, CA, USA) that were placed in groups of up to eight cubes in larger tanks in an aquarium system with circulating artificial seawater (27°C, 12 h:12 h light:dark schedule). Each individual was provided an artificial burrow made of PVC tubing that had been cut longitudinally in half and secured to a corner of the cube with aquarium-safe sealant (i.e. the burrow had only one available opening and the individual was visible from the exterior of the cube). Individuals were fed approximately twice weekly with frozen krill and brine shrimp, or fresh snails. The total number of individuals used in this study, including the number of males and females, is reported in Table 1.

Filming protocol

To conduct a staged contest, we allowed one individual (the 'resident') to remain in its PVC burrow and introduced a competitor (the 'intruder') in a second PVC burrow that was placed directly in front of the opening of the resident's burrow. This introduced burrow was cut in half along its length to allow filming of the contest. Competitors were separated by an opaque barrier until filming began. Before raising the barrier, we ensured both competitors were facing each other. Once the barrier was raised, opponents began interacting, and often sparring, almost immediately.

As competitors sparred, we filmed their strikes (30,000–40,000 frames s^{-1}; high-speed video; Photron SA-Z or SA-X2 camera; 10–15 µs shutter duration; pixel resolution: 1024×512 or 688, SA-Z; 896×496, SA-X2; Photron FastCam Viewer v3; Photron, San Diego, CA, USA). For many contests, we also simultaneously recorded standard digital video (30 frames s^{-1}, Sony Handycam HDR CX-900; Sony Corp., Minato, Tokyo, Japan). These regular-speed videos allowed us to confirm that competitors in staged contests showed similar behaviors to competitors observed in contests from previous studies (Green and Patek, 2015, 2018). For the high-speed filming, we recorded up to three strikes before stopping filming to save the videos. While saving the videos, which took at least 3 min, we separated the competitors to prevent them from further, un-filmed sparring. After saving the videos, we often re-introduced the same competitors (following the same protocol above) to film additional strikes. We used either competitor in up to three 'bouts' (i.e. three consecutive re-introductions), after which we did not use that individual in any contest trials for the rest of the day. All individuals showed consistent competitive behavior throughout the three bouts, suggesting that no individuals were overly fatigued during testing.

After filming contests, we measured each individual's body size and body mass (see below for details on measurement techniques) to ensure competitors were similarly sized. Competitors were within 5% body length of each other, as measured from the anterior tip of the rostral plate to the distal point of the left median apex of the telson (Ahyong, 2001). This body size matching [mean±s.d. percent size difference (min., max.); body length: 4.7±2.8% (0.6, 10.4); body mass: 14.0±10.2% (0.8, 40.0)] is similar to that of previous work on body-length-matched contests in this species (Green and Patek, 2015).

To conduct feeding trials, we fed mantis shrimp snails (*Tritia obsoleta*) that were collected from the Duke University Marine Lab, Beaufort, NC, USA, and maintained at Duke University in an aquarium system with circulating artificial seawater (24°C, 12 h:12 h light:dark schedule). Snails were fed frozen krill or frozen brine shrimp twice weekly.

To film feeding strikes, we first ensured the mantis shrimp were in their PVC burrows. Then, we introduced a snail into the burrow and placed an opaque barrier at the front of the burrow to ensure that the snail and mantis shrimp did not leave the burrow. We did not match snail size to mantis shrimp size following established scaling relationships (Crane et al., 2018; Full et al., 1989), given that we used a different snail species than used in these studies. Instead, we simply gave larger mantis shrimp larger snails than we gave smaller mantis shrimp (see below for a discussion of the effects of size matching). We introduced snails to all individuals at one time and then filmed whichever individual began striking its snail.

Once an individual began striking a snail, we filmed its strikes using the same high-speed camera and imaging settings as for sparring trials. As above, we stopped filming after three recorded strikes to save the videos; however, we did not remove the snail as we were saving videos. Instead, we allowed the mantis shrimp to continue striking and re-started filming as soon as possible. Using

Table 1. Sample sizes and data analyzed in this study

Strike context	No. of individuals (females, males)	No. of strikes	Strikes per individual	Body mass (g)	Max angular velocity (rad s^{-1})	Strike energy (J)	Spring compression (deg)
Total	13 (10, 3)	104	7±3 (4, 15)	1.86±0.74 (0.56, 3.23)	$4.48\times10^3\pm1.92\times10^3$ (1.16×10^3, 1.03×10^4)	0.01±0.01 (0.00, 0.07)	9.9±5.3 (2.2, 27.6)
Sparring	11 (8, 3)	47	4±1 (2, 7)	2.08±0.75 (0.81, 3.23)	$4.82\times10^3\pm1.96\times10^3$ (1.65×10^3, 9.73×10^3)	0.02±0.02 (0.00, 0.07)	12.2±6.4 (2.2, 27.6)
Feeding	9 (8, 1)	57	6±3 (2, 15)	1.69±0.68 (0.56, 2.58)	$4.20\times10^3\pm1.85\times10^3$ (1.16×10^3, 1.03×10^4)	0.01±0.01 (0.00, 0.04)	8.0±3.2 (2.8, 20.2)
Both	7 (6, 1)	63	9±2 (6, 13)	1.64±0.63 (0.78, 2.58)	$4.74\times10^3\pm2.04\times10^3$ (1.59×10^3, 1.03×10^4)	0.01±0.01 (0.00, 0.07)	9.6±5.4 (2.2, 27.6)

The column 'Strikes per individual' reports medians±s.d. (min., max.). Body mass, maximum angular velocity, strike energy and spring compression are reported as means±s.d. (min., max.). The last row ('Both') includes individuals with data for both sparring and feeding strikes. Strike energy and spring compression values were calculated from mathematical modeling; other parameters were measured directly.

still images from these high-speed image sequences, we measured snail size (see 'Morphological measurements') in order to examine how variation in snail size correlated with the kinematics and energetics of mantis shrimp feeding strikes.

Morphological measurements

After filming strikes, we measured each mantis shrimp's body mass (Denver Instruments APX-3202 balance; range: 0–3100 g, readability: 0.01 g, Sartorius AG, Goettingen, Germany) and body length (Mitutoyo Digimatic Caliper, range: 0–150 mm, resolution: 0.01 mm, Mitutoyo Corp., Kawasaki, Japan). We also took standardized photographs of the lateral surface and leading edge of the propodus and dactyl (the 'striking body') using a 12 megapixel digital SLR camera (Nikon D300; AF Micro-NIKKOR 60 mm f/2.8D or 105 mm f/2.8D macro lenses, Nikon Inc., Melville, NY, USA) and an external light source (EM-140 DG macro-flash, Sigma Corp., Ronkonkoma, NY, USA; or Leica KL-300 LED, Leica Corp., Wetzlar, Germany). We took three replicate measurements of body mass and body length, and three replicates of each photograph. Following previous work (e.g. Green and Patek, 2015; Green and Patek, 2018), we used the mean value for each of the three measurements to minimize measurement error.

From the standardized photographs of each individual, we measured three aspects of the shape of the striking body necessary for calculating energetics, as detailed in McHenry et al. (2012): striking body length, average chord width and average thickness (Fiji v.1.50e; Schindelin et al., 2012). Striking body length was measured from the lateral joint of the carpus and propodus to the lateral joint of the propodus and dactyl. Chord width was defined as the width (i.e. perpendicular to the long axis) of the lateral side of the striking body. Average chord width was calculated as the mean value of approximately 20 measurements (range: 16–28, depending on the size of the striking body) taken along the proximal to distal axis of the striking body. Thickness was defined as the lateral to medial distance perpendicular to the long axis of the leading edge of the striking body. Average thickness was calculated as the mean value of approximately 22 measurements along the proximal to distal axis of the leading edge (range: 19–28 measurements, depending on the size of the striking body).

We measured snail size from high-speed video images of 11 out of the total 12 snails fed to mantis shrimp. We isolated images from videos in which the long axis of the snail (apex to the anterior whorl) was in focus. We measured the length, in pixels, of both the long axis of the snail and the longest chord width of the mantis shrimp in the video. We then used the standardized photographs of mantis shrimp appendage morphology to convert the mantis shrimp chord width measurement from pixels to mm. We used this conversion factor (mm pixel^{-1}) to convert our measurements of snail length from pixels to mm. Snail length averaged 10.7 mm (±2.1 mm s.d., range 7.1–14.3 mm). Measurement error, as calculated by the average of the standard deviation of snail length from replicate images of each snail, was approximately 6% (25 total images from 11 snails, median number replicates per snail=2.5, range=1–4 replicates; average s.d. of replicate measurements=0.67 mm).

Digitizing

We digitized appendage motion from the beginning of appendage movement to several frames after contact with the target (either a snail or conspecific) (MtrackJ plugin in Fiji v.1.5.1; Meijering et al., 2012), following methods in Kagaya and Patek (2016). We digitized two points on the striking body and two points on the merus using natural color or brightness patterns on the exoskeleton. To measure the angular displacement of the striking body during a strike, we calculated the relative change in angle between (1) the line formed by the two points on the striking body (points 1 and 2 in Fig. 2A–D) and (2) the line formed by the two merus points (points 3 and 4 in Fig. 2A–D; Kagaya and Patek, 2016). We only digitized videos in which the appendage was visible and remained in focus throughout the strike. In mantis shrimp, strikes that are in focus for the entirety of the strike have minimal digitizing error (deVries et al., 2012). The number of digitized frames for each strike, from the beginning of appendage movement to the frame immediately before contact, was 28±10 frames (mean±s.d.; range: 15–68).

We calculated angular displacement from the raw digitizing data using R code (v. 3.3.2; https://www.r-project.org/) provided in Kagaya and Patek (2016). From the angular displacement data, we then fit seventh- to ninth-order polynomial splines that began at the first movement of the appendage and ended at the frame immediately before contact. For each strike, we fit as high an order of spline as possible (up to ninth-order), following previous studies that used curve fitting for calculations of mantis shrimp strike kinematics (e.g. Cox et al., 2014; deVries et al., 2012). After fitting a spline to the displacement data, we interpolated the spline to gather 5000 time points and 5000 displacement points for each strike. We calculated strike velocity as the derivative of displacement with respect to time and used strike velocity in the energetics modeling described in the next section.

Measurement and modeling of strike energetics

We measured strike energy during contests and feeding through a combination of kinematic measurements and a previously published mathematical model of the mantis shrimp strikes (McHenry et al., 2012). This model equates the elastic potential energy of the raptorial appendage prior to a strike (as determined by spring energy storage and linkage mechanics; McHenry et al., 2012; Patek et al., 2013; Zack et al., 2009) with the kinetic energy of the strike (determined by fluid mechanics; McHenry et al., 2016). We begin this section with a brief overview of the mathematical model (see also Fig. 3) and advise the reader to consult McHenry et al. (2012, 2016) for the full expression of and rationale for the mathematical model.

A strike is powered by the potential energy of a torsion spring (Fig. 3B). Elastic potential energy (E_{spring}) was calculated based on the following relationship:

$$E_{spring} = 0.5k\Delta\theta^2, \quad (1)$$

where k is the torsion spring stiffness (a function of linear spring stiffness and materials testing parameters, see McHenry et al., 2012; Patek et al., 2013; Zack et al., 2009) and $\Delta\theta$ is the spring rotation, relative to its resting position, prior to its release (Fig. 3C).

Strike kinetic energy (E_{KE}) generated by the motion of the appendage was calculated as:

$$E_{KE} = 0.5I\omega^2, \quad (2)$$

where I is the moment of inertia and ω is the angular velocity of the strike (Fig. 3C). The moment of inertia of the striking body and the added mass of the acceleration reaction force was calculated using a blade element approach developed by McHenry et al. (2012) that incorporates measurements of striking body morphology (described above) and the scaling relationship between striking body length and mass (described below; see McHenry et al., 2012 for more details).

Journal of Experimental Biology (2019) 222, jeb198085. doi:10.1242/jeb.198085

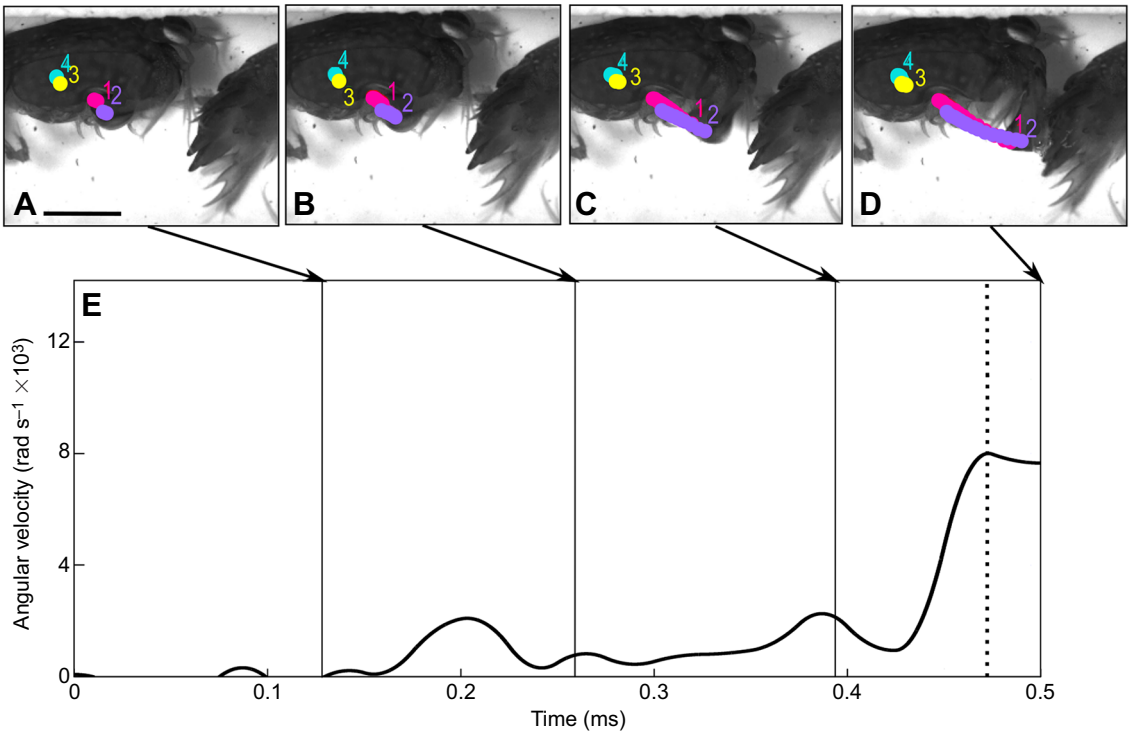

Fig. 2. High-speed videos of strikes were used to quantify raptorial appendage kinematics and were combined with morphological measurements to parameterize a mathematical model of mantis shrimp strike energetics. (A–D) We analyzed strike kinematics using digital image analysis. In this example, we digitized high-speed videos of sparring individuals with two points on the striking body (1: red; 2: purple) and two points on the merus (3: yellow; 4: blue). We measured strike angular velocity (E) from these digitized videos. We used the maximum angular velocity (vertical dotted line in E) and appendage morphology measurements to parameterize a mathematical model predicting kinetic and drag energy (see Materials and Methods). Solid vertical lines in E indicate the corresponding timing for each still image (A–D). Scale bar: 5 mm.

Energy lost to drag (E_{drag}) was calculated as the integral of torque generated by drag (τ) over the total angular position (γ) that the appendage rotates from its starting angle (γ_0):

$$E_{drag} = \int_{\gamma_0}^{\gamma} \tau d\gamma \ . \quad (3)$$

For each measurement of the angular position of the appendage (γ), we calculated kinetic energy (E_{KE}, Eqn 2) and drag energy (E_{drag}, Eqn 3). Drag resists appendage motion to such an extent that velocity, and therefore kinetic energy, reaches a maximum before all of the energy has been released from the spring (McHenry et al., 2012). We performed a series of numerical simulations using McHenry et al.'s (2012) model, which revealed that approximately

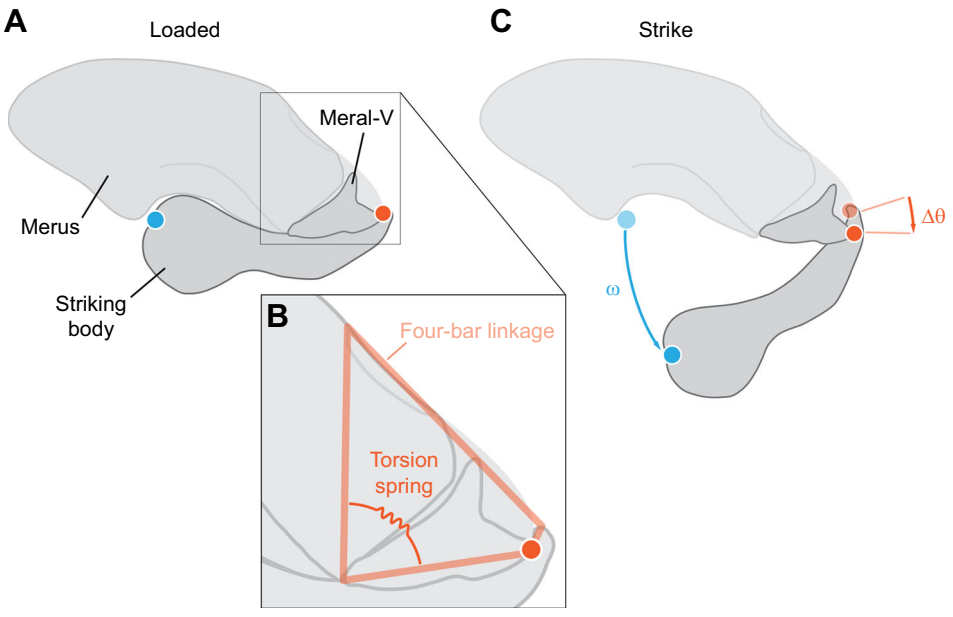

Fig. 3. Spring and strike energy were calculated by modeling the dynamics of the raptorial appendage. (A) According to this model, elastic energy (E_{spring}, Eqn 1) is stored within the merus, which is modeled as a (B) torsion spring at the base of the meral-V. The transmission of torque from the torsion spring to the striking body is provided by a four-bar linkage. The geometry of this linkage determines the gearing of the system and hence the relationship between displacement by the torsion spring ($\Delta\theta$, in red, C) and the striking body. (C) The rate of rotation by the striking body (ω, in blue) during a strike is resisted by the moment of inertia for its mass and the mass of the water (I). Drag provides resistance and causes the system to lose energy (E_{drag}, Eqn 3) and hence the total strike energy (E_{strike}, Eqn 4) is considered the sum of this energy lost and the kinetic energy of the striking body (E_{KE}, Eqn 2).

Journal of Experimental Biology (2019) 222, jeb198085. doi:10.1242/jeb.198085

25% of the initial potential energy remained in the spring at the time of maximum angular velocity. We therefore approximated the total strike energy (E_{strike}) using the following equation:

$$E_{strike} = 1.25E_{KE} + E_{drag}. \quad (4)$$

This calculation was performed at the moment of maximum angular velocity. The 1.25 factor accounts for the potential energy measured at the time of maximum angular velocity as well as the 25% that is unaccounted for at the time of maximum angular velocity.

We calculated E_{strike} using kinematics measured from our high-speed videos (see methods above), as well as the shape and size of the appendages of the experimental animals (also explained above). McHenry et al. (2012) established that the striking body can be modeled as a uniform cylinder with constant material density, and generated a scaling equation for inferring striking body mass from striking body length for a related smasher species, *Gonodactylus smithii* (McHenry et al., 2012). Using these published methods and validations, we calculated the scaling relationship for *N. bredini* by measuring the mass of the propodus and dactyl of both the right and left striking bodies dissected from eight naturally deceased animals (XPE 56 microbalance, resolution: 10^{-6} g, Mettler Toledo Corp., Columbus, OH, USA). This scaling relationship allowed us to infer striking body mass (used in calculations of E_{KE} and E_{drag}) from striking body length. We calculated velocity and energetics for each strike.

Calculations of spring compression

Based on materials testing performed within and across species, spring stiffness does not increase significantly with size, but the distance of spring compression does increase (Patek et al., 2013; Zack et al., 2009). We tested how variation in spring compression relates to variation in E_{strike}. We assumed that our measurements of E_{strike} fully account for E_{spring}, the energy stored in the spring at the beginning of a strike, which powers the outward motion of the strike. Therefore, we set E_{strike}=E_{spring} and solved Eqn 1 for $\Delta\theta$:

$$\Delta\theta = \sqrt{\frac{2E_{strike}}{k}}. \quad (5)$$

We set k, the torsion spring stiffness, equal to average *N. bredini* spring stiffness as measured in Patek et al. (2013). Because k was originally measured as a linear spring, we converted it to torsion spring stiffness following McHenry et al. (2012). For each value of E_{strike} from our kinematics-based dataset, we used Eqn 5 to solve for $\Delta\theta$. This analysis does not incorporate how variation in other aspects of the spring system, such as the scaling of link lengths (Anderson and Patek, 2015), might influence variation in E_{spring}.

Statistical analyses

We tested how strike velocity and strike energy (E_{strike}) separately scale with body mass using linear mixed models (LMMs; lmer function, lme4 package, R v. 3.0.1; Bates et al., 2015). We first determined which variables should be included as random effects by testing whether they significantly improved the fit of models predicting strike energy from body mass. A better-fit model was one that had a ΔAIC of less than −2 [lower Akaike information criterion (AIC) scores were better fit; ANOVA function in R]. In all cases, we included individual ID as a random effect to control for taking multiple measurements from each individual. We tested for random effects of (1) date of high-speed video recording (as Julian date), (2) fit of the polynomial spline for each strike (seventh-, eighth- or ninth-order), (3) order the strike was delivered in the recording sequence (e.g. first, second, third, …*n*th strike recorded from each individual in a given sparring or feeding bout) and (4) order of the bout (e.g. first, second, third time an individual was paired with a competitor). Spline fit, strike order and bout order had no significant effect on the results and were therefore not included as random effects. Including recording date significantly improved model fit, potentially reflecting seasonal or age-related changes within individuals across the time frame of the study. We included recording date (1|date) and individual ID (1|ID) as random effects in all models.

To test whether maximum angular velocity (ω_{max}) scaled with body mass for sparring and/or feeding strikes, our LMM structure was:

$$\log_{10}(\omega_{max}) \sim \log_{10}(\text{body mass}) \times \text{strike context} + (1|\text{date}) + (1|\text{ID}), \quad (6)$$

where strike context was either sparring or feeding. To test whether strike energy (E_{strike}) scaled with body mass for sparring and/or feeding strikes, our LMM structure was:

$$\log_{10}(E_{strike}) \sim \log_{10}(\text{body mass}) \times \text{strike context} + (1|\text{date}) + (1|\text{ID}). \quad (7)$$

For both models, we tested whether scaling relationships differed between sparring and feeding strikes by comparing the fit of the full model with a model in which we did not include strike context (i.e. a model that grouped all strikes together). For each strike context, we also tested whether the scaling relationships were significantly different from zero. We split our full dataset into two separate subsets: one for only sparring strikes and one for only feeding strikes. Then, for each of these datasets, we tested whether the fit of models that included size and random effects was better than models with only random effects (i.e. models that did not account for size variation). Because we were testing the hypothesis that slopes were significantly different from zero (as opposed to simply comparing models), we used the χ^2 values and associated P-values from likelihood ratio tests to test for significance.

We examined how variation in spring compression related to the scaling of E_{spring} by plotting $\Delta\theta$ (in degrees) as a second y-axis in the scaling relationships for E_{trike}. To test whether the variation in spring compression was different between sparring and feeding strikes, we took the mean value of spring compression for each individual and each strike context (sparring or feeding) and tested for unequal variance using the leveneTest function in the car package in R (Fox and Weisberg, 2011).

Post hoc analyses: the effects of relative size on kinematics and energetics

Although the present experiment was not designed to test how individuals alter kinematics or energetics based on their own size relative to that of their competitor or their prey, this factor could have influenced scaling relationships. Therefore, we conducted *post hoc* tests to establish how strike kinematics and energetics were affected by relative opponent size (for sparring strikes) and relative prey size (for feeding strikes).

Sparring strikes

We reduced the original dataset into a new dataset containing only those sparring strikes for which we had data on opponent body mass

Journal of Experimental Biology (2019) 222, jeb198085. doi:10.1242/jeb.198085

(9 of 11 individuals). Then, we established a measurement of relative mass, defined as the mass of the focal individual relative to its opponent (Briffa et al., 2013):

$$\text{Relative mass} = 1 - \left(\frac{\text{opponent mass}}{\text{focal mass}}\right). \quad (8)$$

Relative mass is a predictor of contest success in *N. bredini*, such that individuals with higher relative mass are more likely to win contests (Green and Patek, 2018).

We first tested whether relative mass was significantly affected by focal body mass, which would occur if larger or smaller individuals were matched with relatively larger or smaller opponents more often than expected by chance. We fit an LMM of the form:

$$\text{Relative mass} \sim \text{body mass} + (1|\text{date}) + (1|\text{ID}), \quad (9)$$

and tested whether this model was a better fit than a model including only random effects. If larger or smaller individuals were preferentially matched with larger or smaller opponents, then the model including body mass would be a better fit than the model with only random effects.

To test whether relative mass influenced the maximum angular velocity or strike energy of strikes, we built mixed models of the form:

$$\log_{10}(\omega_{max}[\text{or } E_{strike}]) \sim \log_{10}(\text{body mass}) + \text{relative mass} + (1|\text{date}) + (1|\text{ID}). \quad (10)$$

We tested whether the full model (i.e. including relative mass) was a better predictor of strike maximum angular velocity or strike energy than models that did not include relative mass.

Feeding strikes

To test for the effect of relative prey size on strike scaling, we first calculated relative snail size as the ratio of snail length to mantis shrimp body mass. Then, to establish whether relative snail size differed across mantis shrimp body mass (i.e. whether larger or smaller mantis shrimp were preferentially given larger or smaller snails), we fit an LMM of the form:

$$\text{Relative snail size} \sim \text{body mass} + (1|\text{date}) + (1|\text{ID}), \quad (11)$$

and tested whether this model was a better fit than a model including only random effects.

Next, using similar LMM analyses as our test of relative competitor matching, we tested whether maximum angular velocity or strike energy scaling were associated with relative snail size. We fit an LMM of the form:

$$\log_{10}(\omega_{max}[\text{or } E_{strike}]) \sim \log_{10}(\text{body mass}) + \text{relative snail size} + (1|\text{date}) + (1|\text{ID}), \quad (12)$$

and tested whether this model was a better fit to our data than a model that did not include relative snail size.

RESULTS

Strike velocity

The best fit model predicting strike maximum angular velocity included both body mass and strike context (sparring or feeding) as fixed effects, with recording date and individual ID as random effects (Table 2). Maximum angular velocity did not scale with body mass for sparring strikes (slope=0.13, N=11 individuals, 47 strikes) and scaled negatively with mass for feeding strikes (slope=−0.73, N=9 individuals, 57 strikes; Table 2, Fig. 4). Individuals in the upper quartile of body mass delivered sparring strikes with 90% of the mean maximum angular velocity of those in the lower quartile of body mass (upper quartile mean±s.d.=$3.98\times10^3\pm1.95\times10^3$ rad s^{-1}, N=2 individuals, 12 strikes; lower quartile mean±s.d.=$4.44\times10^3\pm1.81\times10^3$ rad s^{-1}, N=4 individuals, 15 strikes). For feeding strikes, these larger individuals struck with only 50% of the maximum angular velocity of smaller individuals (upper quartile mean ±s.d.=$2.83\times10^3\pm1.02\times10^3$ rad s^{-1}, N=3 individuals, 20 strikes; lower quartile mean±s.d.=$5.71\times10^3\pm1.70\times10^3$ rad s^{-1}, N=3 individuals, 17 strikes).

Strike energy and spring compression

The best fit model predicting strike energy included both body mass and strike context (sparring or feeding) as fixed effects, with recording date and individual ID as random effects (Table 2). Strike energy scaled positively with body mass for sparring strikes (slope=2.13, N=11 individuals, 47 strikes) and did not scale with mass for feeding strikes (slope=0.12, N=9 individuals, 57 strikes; Table 2, Fig. 5). For sparring strikes, individuals in the upper quartile of body mass struck with 230% the energy of those in the lower quartile of body mass (upper quartile mean±s.d.=0.02±0.01 J, N=2 individuals, 12 strikes; lower quartile mean±s.d.=0.01±0.01 J, N=4 individuals, 15 strikes). This relative value was only 119% for feeding strikes (upper quartile mean±s.d.=0.01±0.00 J, N=3 individuals, 20 strikes; lower quartile mean±s.d.=0.01±0.00 J, N=3 individuals, 17 strikes).

Table 2. Results of statistical models testing the effects of body size and behavioral context on strike velocity and energy

Behavior	Dependent variable	Fixed effect(s)	Model AIC (random effects AIC)	χ^2, d.f. (P-value)	Model equation	
					Slope	Intercept
Velocity						
All	$\log_{10}$ (Maximum angular velocity)	$\log_{10}$ (Body mass) Strike context	−56.07 (−48.91)	–	–	
Sparring	$\log_{10}$ (Maximum angular velocity)	$\log_{10}$ (Body mass)	–	0.26, 1 (0.61)	0.13	3.6
Feeding	$\log_{10}$ (Maximum angular velocity)	$\log_{10}$ (Body mass)	–	*7.57, 1 (<0.01)*	−0.73	3.7
Strike energy						
All	$\log_{10}$ (Strike energy)	$\log_{10}$ (Body mass) Strike context	106.80 (120.65)	–	–	
Sparring	$\log_{10}$ (Strike energy)	$\log_{10}$ (Body mass)	–	*4.30, 1 (0.04)*	2.13	−2.66
Feeding	$\log_{10}$ (Strike energy)	$\log_{10}$ (Body mass)	–	1.90, 1 (0.17)	0.12	−2.40

Each model was analyzed in terms of velocity, strike energy and strike context used in the model (feeding, sparring or all data combined). For models run with the 'All' behavior, we used AIC scores to compare the fit of a full model with that of a model without the effect of strike context (feeding or sparring). For every model, we included random effects of Julian date and individual ID. For models run with 'Feeding' or 'Sparring' behaviors, we tested whether the slope of the model equation was different from zero using χ^2 values and P-values from likelihood ratio tests. Significant P-values (<0.05) are indicated by italics.

Journal of Experimental Biology (2019) 222, jeb198085. doi:10.1242/jeb.198085

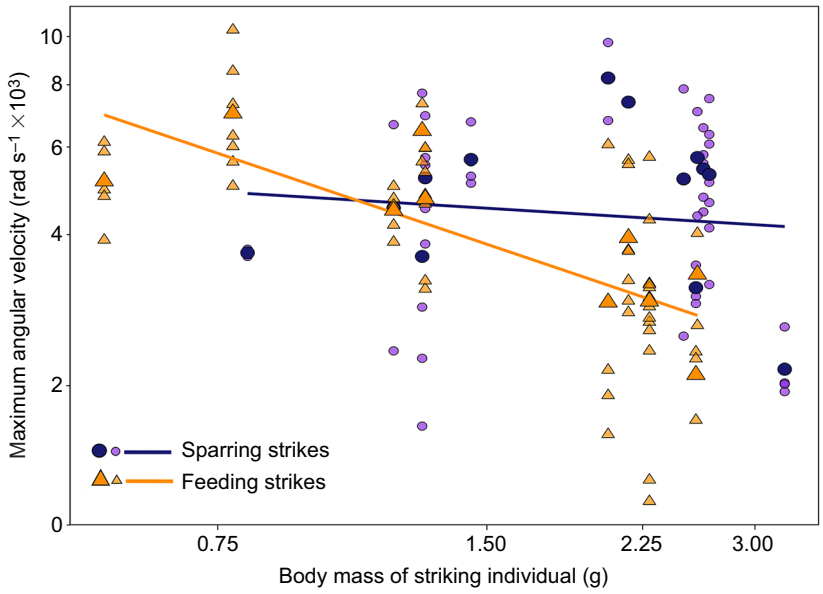

Fig. 4. Sparring strike velocity (purple) does not consistently vary with body mass of the striking individual, whereas feeding strike velocity (orange) decreases with increasing body mass. The small light-shaded symbols represent individual strikes and the larger dark-shaded symbols represent means for each individual. Axes are $\log_{10}$–$\log_{10}$. Correlation lines are taken from simple linear models and do not include random effects of filming date or individual ID. Statistical results from linear mixed models including these random effects are reported in Table 2.

Variation in energy was approximately equally distributed between kinetic and drag energy, as shown by LMMs of the full dataset that included random effects but did not include a fixed effect of strike context. There were similar scaling relationships between $\log_{10}$-transformed body mass and $\log_{10}$-transformed strike energy (slope=1.10, intercept=−2.44, N=13 individuals, 104 strikes), $\log_{10}$-transformed kinetic energy (slope=1.08, intercept=−2.80) and $\log_{10}$-transformed drag energy (slope=1.18, intercept=−2.84).

Using our measurements of strike energy, we calculated that spring compression for the strikes we measured varied from 2.2 to 27.6 deg (Fig. 5, Table 1). The variation in mean spring compression for sparring strikes was significantly greater than that of feeding strikes (sparring strike range=2.2–27.6 deg; feeding strike range=2.8–20.2 deg; Levene test $F_{1,18}$=6.36, P=0.02; sparring strikes: N=11 individuals, 47 strikes; feeding strikes: N=9 individuals, 57 strikes).

Post hoc analyses: effects of relative opponent and prey size

In our *post hoc* analyses of the effects of relative opponent size, we first found that the full model predicting relative mass from both focal individual mass and random effects was not a better fit than the model including only random effects (full model AIC=−114.11, ΔAIC from the model including only random effects=1.95, N=9 individuals). Therefore, relative mass did not show significant directional variation over our range of focal individual body size. Relative opponent mass was included in the model that best predicted sparring strike maximum angular velocity (AIC=−12.22; ΔAIC from model without relative mass=−4.98, N=9 individuals, 34 strikes). The slope estimate of the relative mass effect (−0.76) showed that focal individuals that were relatively larger than their opponents struck with lower velocity than focal individuals that were relatively smaller than their opponents. The model including relative mass was also the best predictor of sparring strike energy (AIC: 44.30; ΔAIC from model without relative mass=−7.33). The

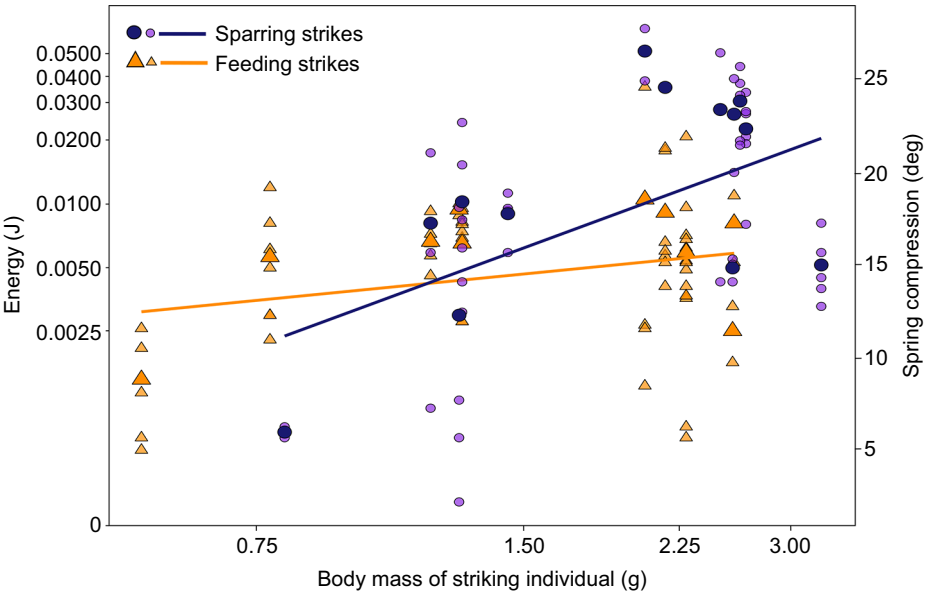

Fig. 5. When sparring, strike energy (purple) scales positively with body mass, whereas during feeding, strike energy (orange) does not scale with body mass. Spring compression increases with increasing strike energy. Light-shaded circles and triangles represent individual strikes; dark-shaded circles and triangles represent means for each individual's body mass. Axes are $\log_{10}$–$\log_{10}$, except for spring compression (right y-axis). Correlation lines are taken from simple linear models and do not include random effects of filming date or individual ID. Statistical results from linear mixed models including these random effects are reported in Table 2.

slope estimate of the relative mass effect (−2.23) showed that focal individuals that were relatively larger than their opponents used less energy in sparring strikes than focal individuals that were relatively smaller than their opponents.

When analyzing the effects of relative snail size, we first found that the full model predicting relative snail size from both mantis shrimp body mass and random effects was a better fit than the model including only random effects (full model AIC=−504.16, ΔAIC from model including only random effects=−74.36, N=8 mantis shrimp, 10 snails). The slope of the mass effect (−0.69) indicated that larger mantis shrimp were fed proportionally smaller snails than smaller mantis shrimp. When analyzing the effects of relative snail size on strike kinematics and energetics, we found that the LMM including relative snail size was not a better fit to the data than a model that did not include relative snail size for either maximum angular velocity (full model AIC=−10.59, ΔAIC from model without relative size=−0.18, N=8 mantis shrimp, 10 snails, 53 strikes) or strike energy (full model AIC=28.51, ΔAIC from model without relative size=−0.75). Therefore, although relative snail size differed between smaller and larger mantis shrimp, it is unlikely that this factor influenced the scaling results.

DISCUSSION

This study establishes that the scaling of strike velocity and energetics differs between the two behavioral contexts of sparring and feeding. During sparring behaviors, strike velocity did not change with the mass of the striking individual, whereas strike energy increased with mass (Figs 4, 5, Table 2). For feeding strikes, velocity scaled negatively with body mass and energy did not scale with mass (Figs 4, 5, Table 2). Larger individuals exhibited greater strike energy while sparring, but not while feeding, by generating greater spring compression prior to a strike (Fig. 5). Finally, the relative mass of competitors, but not prey, affected the scaling of strike kinematics and energetics. Our results reveal how variation in the kinematics and energetics of a spring-powered motion may be controlled according to behavioral context.

Scaling principles of kinematics and energetics

At the level of the individual, a faster strike is more energetically costly, and variation in strike velocity may represent varying effort. However, across a range of individual sizes, faster strikes do not necessarily require more energy. This connection between kinematics (velocity) and energetics is fundamental to understanding the scaling relationships discovered in this study. Energy is calculated based on strike velocity and the size and mass of the appendage (Eqns 1–4; Fig. 3). Increases in size incur energetic costs for both kinetic energy (owing to increased moment of inertia) and drag energy, which resists movement of the appendage through water. We found that drag energy and kinetic energy made approximately equal contributions to the scaling of strike energy (see Results). This suggests that both inertial and hydrodynamic resistance are important in governing the scaling of kinematics and energetics.

The size dependence of strike mechanics (McHenry et al., 2012) illuminates why strike velocity (Fig. 4) and strike energy (Fig. 5) can exhibit distinct scaling relationships that reflect both individual body size and individual effort. For example, larger sparring individuals struck with velocities similar to those of smaller individuals (Fig. 4), but, in doing so, they incurred higher energetic costs (Fig. 5). Likewise, larger feeding individuals struck more slowly than smaller individuals (Fig. 4), resulting in an energy output that did not vary with size (Fig. 5).

In this context of mechanical scaling, our results also indicate how behavior can mediate differences in velocity and energetics with size. Even within the constraints of the unchangeable energetic effects of their body size, individuals can adjust their strike velocity and, therefore, their energetic output. This is evident through the computed spring compression necessary to adjust energetic output: increased energetic output required greater spring compression in preparation for sparring strikes (Fig. 5). That spring compression varied less with body size in feeding strikes supports the conclusion that individuals adjusted their energetic input depending on the behavioral context. Validating these modeling results, previous direct measurements of spring compression documented a similar range of angles (mean: 8 deg; range: 1–26 deg; Kagaya and Patek, 2016).

Contests

The finding that sparring energy scaled positively with body mass fits with the current understanding of *N. bredini* contest behavior and suggests a communicative function for energetics in this system. Telson sparring and other contest behaviors match the predictions of mutual assessment models of contest behavior, in which competitors gauge their own and their competitor's ability (Green and Patek, 2018). Ability in these contests is related to mass, such that larger individuals have a competitive advantage (Green and Patek, 2018). Size assessment via striking may be advantageous in *N. bredini*, as visual assessment may be difficult: contests often occur in enclosed, dark burrows where competitors' bodies are hidden by their coiled, protective telsons (P.A.G., personal observation). The present study suggests that receivers of strikes could potentially use the energy of an opponent's strike to inform size-based assessment. For example, higher-energy strikes produced by larger individuals could result in greater deformation of the telson, which could be sensed by the receiver of the strike. This interpretation assumes that competitors consistently deliver sparring strikes at maximum strike energy. Size assessment via sparring may also be possible for the striking individual. The telson's ability to dissipate strike energy scales positively with body mass; only the telson behaves this way – the nearby abdominal exoskeleton does not exhibit dissipation scaling with body size (Taylor and Patek, 2010). Because of this, striking individuals could potentially assess competitor size through this dissipation of strike energy (Taylor and Patek, 2010). Our *post hoc* tests showing that individuals used lower-velocity, lower-energy strikes against relatively smaller opponents also suggest that striking individuals may use strikes to assess opponent size and alter strike velocity and energetics accordingly. The results of our *post hoc* tests should be considered in the context of the relatively low sample size (nine individuals) – a consequence of the fact that this analysis was not part of the original experimental design. Future work could use controlled manipulations of competitor size, with a larger sample size, to better test how strike velocity and energetics shift as a result of within-contest assessment.

Feeding

Smaller mantis shrimp struck snails with greater velocity and with a similar amount of energy as larger mantis shrimp. Our *post hoc* test found that although smaller mantis shrimp fed on proportionally larger snails, this was not associated with changes in strike velocity and energetics. Possibly, *N. bredini* have lower motivation during feeding than contests, especially for larger individuals. Feeding *N. bredini* take an average of 73 strikes to open snails (Crane et al., 2018), whereas size-matched *N. bredini* contests involve an average

of only five strikes (Green and Patek, 2018). It may be more important for competing mantis shrimp to strike with maximum energy during sparring, as the ultimate outcome (winning or losing) depends on fewer strikes. In the feeding experiments, individuals were also isolated in their protective burrows for as long as needed to process prey – conditions that may facilitate low-stakes, low-energy striking. These conditions may be similar to mantis shrimp feeding in their protective natural burrows in the wild; however, they could be interrupted by intruding competitors or predators. To better understand the drivers of variation in feeding strike velocity and energetics, future studies could present different snail sizes relative to mantis shrimp size to test whether velocity and/or energy use changes according to the size or armor of prey.

Spring compression

Mantis shrimp adjust their spring-driven strikes based on behavioral context. Our estimates of spring compression demonstrated that larger individuals compressed the spring more than smaller individuals when sparring, but spring compression was fairly constant across individual sizes during feeding (Fig. 5). The parameters used in our model matched previous research that found a positive correlation between spring compression and body size, even though spring stiffness remains similar across the same size range (Patek et al., 2013; Zack et al., 2009). Although other aspects of the strike mechanism, such as the link lengths of the four-bar linkage system (Anderson et al., 2014; Patek et al., 2004, 2007), may change across a size range, we kept these variables constant for simplicity. Future work could test whether altering these and other parameters change scaling dynamics.

We were unable to test whether the relationships between spring compression and behavioral context were related to physical limitation, motivation or both. Larger *N. bredini* compressed their spring to a greater degree than smaller *N. bredini* during sparring, but not while feeding. Given that larger animals can compress the spring to a greater degree than smaller animals (Patek et al., 2013; Zack et al., 2009), maximal spring compression would be evident as a positive correlation between body size and spring compression. In contrast, while feeding, smaller individuals used the same spring compression as larger individuals. Perhaps larger individuals were less motivated than smaller individuals while feeding, or they simply did not need to compress their spring maximally to deliver sufficient energy to open prey. While sparring, all individuals were potentially equally motivated, which may be related to size-based signaling in this system (see above). Direct measurements of spring compression during these behaviors are necessary to fully parse these explanations.

The finding that variation in spring compression relates to energetic scaling has relevance to behavior in this and other spring-driven systems. Adjustment of spring compression prior to a strike is a key component of 'behavioral control' in the mantis shrimp strike. Because the strike is so brief, individuals cannot alter strike kinematics once the appendage is released; however, before a strike, they can contract their muscles to achieve greater or lesser spring compression (Kagaya and Patek, 2016). Understanding how animals control spring-powered movements is an important topic in biomechanics (Ilton et al., 2018; Rosario et al., 2016); our results lend insight into both how (spring compression) and why (behavioral context) animals alter these movements.

Comparisons with whole-body energetics

Previous measurements of *N. bredini* whole-body energetics help place our mathematical modeling-based results in context. Full et al. (1989) used carbon dioxide production as a proxy for energy metabolism in *N. bredini*. In addition to measuring resting metabolic rate (RMR), they also calculated the energy needed to deliver feeding strikes to *Tegula* spp. snails by (1) measuring CO_2 production during feeding, (2) subtracting the metabolic cost of handling and manipulating prey, and (3) dividing by the frequency of striking (Full et al., 1989). Taking their results into account, our measurements suggest that each sparring strike required, on average, approximately 1% of hourly RMR, while each feeding strike required an average of 0.5% of hourly RMR. Our approach also revealed that the energy required to deliver a feeding strike was approximately one-third of that calculated by Full et al. (1989).

These comparisons reveal differences in the energetic cost of striking when using biomechanics-based techniques (present study) versus techniques based on CO_2 production (Full et al., 1989). This might be expected: whereas our approach measured strike energetics directly from kinematics, Full et al. (1989) took whole-body CO_2 production measurements and statistically removed the energetic costs of non-strike metabolism to determine a strike-based cost. Future work could measure both CO_2 production and other energetic proxies such as lactate production or *in vitro* muscle work, and then compare those estimates with kinematics-based energy measurements. This multi-pronged approach would enable critical assessment of both experimental techniques and ultimately converge on precise estimates of energetic costs.

Our comparison of the energetics of sparring strikes with the hourly RMR measurements of Full et al. (1989) also relates to work suggesting that many sexually selected behaviors have lower energetic costs than expected. From mate choice displays (e.g. Barske et al., 2014) to contest behaviors (e.g. Boisseau et al., 2017; Reichert, 1988), many studies have found low energetic costs of sexually selected behaviors. We found that sparring strikes require only 1% of hourly RMR (as measured by Full et al., 1989), though we did not measure the costs of other movements involved in sparring, such as coiling the telson in front of the body, or any neural costs of assessment or delivering strikes. Recent reviews suggest that honest signaling systems can be maintained by non-energetic costs, including socially enforced costs such as competitive retaliation for cheating (Searcy and Nowicki, 2005; Számadó, 2011). Although socially enforced costs are currently untested in *N. bredini*, our findings support recent work suggesting that energetic costs may not be the sole enforcer of signal honesty in some animal communication systems.

Energetics and effort in context

Although we did not directly measure animal performance (*sensu* Arnold, 1983), our comparisons of velocity and energetics across the contexts of feeding and sparring may inform studies of animal performance. Many performance measurements are conducted in laboratory conditions, for example by placing a force sensor inside the animal's jaws or claws, or directly in front of the animal, until it bites, grasps or strikes (Franklin et al., 2019; Green and Patek, 2015; Huber et al., 2005; Husak et al., 2006; Lappin et al., 2006; Wilson et al., 2007). These measurement conditions are both motivationally and mechanically distinct from the scenarios in which the animal performs its ecologically relevant activity (Arnold, 1983). Motivationally, performance is measured in a different behavioral context (e.g. while being handled by a researcher, not while in a contest or while feeding); mechanically, researchers ensure proper measurement technique (e.g. force plate alignment), which is likely not comparable to the conditions of the actual task.

When we allowed mantis shrimp to compete or feed freely (i.e. without handling by us), we found that behavioral context was

associated with different strike kinematics and energetics. Sparring strikes were, on average, faster and more energetically costly than feeding strikes. Across our sample, the mean value of sparring strike maximum angular velocity was 1.15 times that of feeding strikes (Table 1). After accounting for body mass variation, the mean value of sparring strike energy was 1.82 times that of feeding strikes (Table 1). Additionally, although mantis shrimp in the largest quartile of body mass delivered sparring strikes with 90% the velocity and 230% the energy of mantis shrimp in the smallest quartile of body mass, they struck prey with only 50% the velocity and 119% the energy of these smaller mantis shrimp (see Results).

A central and often exceptionally challenging goal of organismal biology is to measure animal performance in real behavioral contexts (Losos et al., 2002). Recent studies have used movement-based analyses to test how performance influences contest success (Briffa and Fortescue, 2017) or mate choice (Barske et al., 2011), or to ask how theories of sexual selection can be informed by performance measurements (Byers et al., 2010; Manica et al., 2017; Schuppe and Fuxjager, 2018). Our study contributes new evidence and approaches to reveal how the energy animals invest in powering movement can change with behavioral context.

Acknowledgements
We thank R. Crane, M. S. deVries, G. Farley, J. Harrison and C. Kuo for help collecting mantis shrimp and snails, and members of the Patek Lab for feedback and ideas. The staff at the Smithsonian Tropical Research Institute (STRI), especially the Galeta Marine Laboratory, contributed valuable assistance and facilities. A. Bhatt and B. Sauer helped with filming and digitizing mantis shrimp strikes. M. Zipple provided statistical advice. E. Caves, S. Johnsen, S. Nowicki, D. Pfennig, V. L. Roth and A. Summers gave feedback on design, analysis and writing.

Competing interests
The authors declare no competing or financial interests.

Author contributions
Conceptualization: P.A.G., S.N.P.; Methodology: P.A.G., S.N.P., M.J.M.; Software: P.A.G., S.N.P., M.J.M.; Validation: P.A.G., S.N.P., M.J.M.; Formal analysis: P.A.G., M.J.M.; Investigation: P.A.G.; Resources: P.A.G., S.N.P.; Data curation: P.A.G., M.J.M.; Writing - original draft: P.A.G.; Writing - review & editing: P.A.G., S.N.P., M.J.M.; Visualization: P.A.G., S.N.P., M.J.M.; Supervision: P.A.G., S.N.P.; Project administration: P.A.G., S.N.P.; Funding acquisition: P.A.G., S.N.P.

Funding
This research was funded by a National Science Foundation grant (IOS 1439850) to S.N.P., a National Science Foundation grant (IOS 1354842) to M.J.M. and a Duke University Biology Fellowship, Grants in Aid and Summer Research Fellowship to P.A.G.

Data availability
Data are available from the Dryad Digital Repository (Green et al., 2019): https://doi.org/10.5061/dryad.d4m3986

References
Ahyong, S. T. (2001). *Revision of the Australian Stomatopod Crustacea*. Sydney: Australian Museum.
Anderson, P. S. L. and Patek, S. N. (2015). Mechanical sensitivity reveals evolutionary dynamics of mechanical systems. *Proc. R. Soc. B* **282**, 20143088.
Anderson, P. A. L., Claverie, T. and Patek, S. N. (2014). Levers and linkages: mechanical tradeoffs in a power-amplified system. *Evolution* **68**, 1919-1933.
Arnold, S. J. (1983). Morphology, performance and fitness. *Am. Zool.* **23**, 347-361.
Barske, J., Schlinger, B. A., Wikelski, M. and Fusani, L. (2011). Female choice for male motor skills. *Proc. R. Soc. B* **278**, 3523-3528.
Barske, J., Fusani, L., Wikelski, M., Feng, N. Y., Santos, M. and Schlinger, B. A. (2014). Energetics of the acrobatic courtship in male golden-collared manakins (*Manacus vitellinus*). *Proc. R. Soc. B* **281**, 20132482.
Bates, D., Mäechler, M., Bolker, B. and Walker, S. (2015). Fitting linear mixed-effects models using lme4. *J. Stat. Softw.* **67**, 1-48.
Boisseau, R. P., Woods, H. A. and Goubault, M. (2017). The metabolic costs of fighting and host exploitation in a seed-drilling parasitic wasp. *J. Exp. Biol.* **220**, 3955-3966.
Briffa, M. and Elwood, R. W. (2001). Decision rules, energy metabolism, and vigour of hermit-crab fights. *Proc. R. Soc. B* **268**, 1841-1848.
Briffa, M. and Fortescue, K. J. (2017). Motor pattern during fights in the hermit crab *Pagurus bernhardus*: evidence for the role of skill in animal contests. *Anim. Behav.* **128**, 13-20.
Briffa, M. and Sneddon, L. U. (2007). Physiological constraints on contest behaviour. *Funct. Ecol.* **21**, 627-637.
Briffa, M., Hardy, I. C. W., Gammell, M. P., Jennings, D. J., Clarke, D. D. and Goubault, M. (2013). Analysis of animal contest data. In *Animal Contests* (ed. I. C. W. Hardy and M. Briffa), pp. 47-85. Cambridge University Press.
Burrows, M. (1969). The mechanics and neural control of the prey capture strike in the mantid shrimps *Squilla* and *Hemisquilla*. *Zeitschrift für vergleichende Physiologie* **62**, 361-381.
Burrows, M. and Hoyle, G. (1972). Neuromuscular physiology of the strike mechanism of the mantis shrimp, *Hemisquilla*. *Zeitschrift für vergleichende Physiologie* **179**, 379-394.
Byers, J., Hebets, E. and Podos, J. (2010). Female mate choice based upon male motor performance. *Anim. Behav.* **79**, 771-778.
Caldwell, R. L. (1987). Assessment strategies in stomatopods. *Bull. Mar. Sci.* **41**, 135-150.
Caldwell, R. L. and Dingle, H. (1975). Ecology and evolution of agonistic behavior in stomatopods. *Naturwissenschaften* **62**, 214-222.
Caldwell, R. L., Roderick, G. K. and Shuster, S. M. (1989). Studies of predation by *Gonodactylus bredini*. In *Biology of Stomatopods: Selected Symposia and Monographs* (ed. E. A. Ferrero), pp. 117-131. Mucchi, Modena: Unione Zoologica Italiana.
Clark, C. J. (2012). The role of power versus energy in courtship: what is the 'energetic cost' of a courtship display? *Anim. Behav.* **84**, 269-277.
Cox, S. M., Schmidt, D., Modarres-Sadeghi, Y. and Patek, S. N. (2014). A physical model of the extreme mantis shrimp strike: kinematics and cavitation of Ninjabot. *Bioinspir. Biomim.* **9**, 1-16.
Crane, R. L., Cox, S. M., Kisare, S. A. and Patek, S. N. (2018). Smashing mantis shrimp strategically impact shells. *J. Exp. Biol.* **221**, 1-11.
DeCarvalho, T. N., Watson, P. J. and Field, S. A. (2004). Costs increase as ritualized fighting progresses within and between phases in the sierra dome spider, *Neriene litigiosa*. *Anim. Behav.* **68**, 473-482.
deVries, M. S., Murphy, E. A. and Patek, S. N. (2012). Strike mechanics of an ambush predator: the spearing mantis shrimp. *J. Exp. Biol.* **215**, 4374-4384.
deVries, M. S., Stock, B. C., Christy, J. H., Goldsmith, G. R. and Dawson, T. E. (2016). Specialized morphology corresponds to a generalist diet: linking form and function in smashing mantis shrimp crustaceans. *Oecologia* **182**, 429-442.
Dingle, H. (1969). A statistical and information analysis of aggressive communication in mantis shrimp *Gonodactylus bredini* Manning. *Anim. Behav.* **17**, 561-575.
Dingle, H. and Caldwell, R. L. (1969). The aggressive and territorial behaviour of the mantis shrimp *Gonodactylus bredini* Manning (Crustacea: Stomatopoda). *Behaviour* **33**, 115-136.
Fox, J. and Weisberg, S. (2011). *An R Companion to Applied Regression*. Thousand Oaks, CA: Sage.
Franklin, A. M., Donatelli, C. M., Culligan, C. R. and Tytell, E. D. (2019). Meral-spot reflectance signals weapon performance in the mantis shrimp *Neogonodactylus oerstedii* (Stomatopoda). *Biol. Bull.* **236**, 43-54.
Full, R. J., Caldwell, R. L. and Chong, S. W. (1989). Smashing energetics: prey selection and feeding efficiency of the stomatopod, *Gonodactylus bredini*. *Ethology* **81**, 134-147.
Green, P. A. and Patek, S. N. (2015). Contests with deadly weapons: telson sparring in mantis shrimp (Stomatopoda). *Biol. Lett.* **11**, 1-4.
Green, P. A. and Patek, S. N. (2018). Mutual assessment during ritualized fighting in mantis shrimp (Stomatopoda). *Proc. R. Soc. B* **285**, 20172542.
Green, P. A., Patek, S. N. and McHenry, M. J. (2019). Data from: Context-dependent scaling of kinematics and energetics during contests and feeding in mantis shrimp. Dryad Digital Repository. https://doi.org/10.5061/dryad.d4m3986
Hack, M. A. (1997). The energetic costs of fighting in the house cricket, *Acheta domesticus* L. *Behav. Ecol.* **8**, 28-36.
Huber, D. R., Eason, T. G., Hueter, R. E. and Motta, P. J. (2005). Analysis of the bite force and mechanical design of the feeding mechanism of the durophagous horn shark *Heterodontus francisci*. *J. Exp. Biol.* **208**, 3553-3571.
Husak, J. F., Lappin, A. K., Fox, S. F. and Lemos-Espinal, J. A. (2006). Bite-force performance predicts dominance in male venerable collard lizards (*Crotaphytus antiquus*). *Copeia* **2006**, 301-306.
Ilton, M., Bhamla, M. S., Ma, X., Cox, S. M., Fitchett, L. L., Kim, Y., Koh, J.-S., Krishnamurthy, D., Kuo, C.-Y., Temel, F. Z. et al. (2018). The principles of cascading power limits in small, fast biological and engineered systems. *Science* **360**, 1-11.
Kagaya, K. Patek, S. N. (2016). Feed-forward motor control of ultrafast, ballistic movements. *J. Exp. Biol.* **219**, 319-333.
Lappin, A. K., Brandt, Y., Husak, J. F., Macedonia, J. M. and Kemp, D. J. (2006). Gaping displays reveal and amplify a mechanically-based index of weapon performance. *Am. Nat.* **168**, 100-113.

Losos, J. B., Creer, D. A. and Shulte, J. A. I. (2002). Cautionary comments on the measurement of maximum locomotor capabilities. *J. Zool.* **258**, 57-61.
Manica, L. T., Macedo, R. H., Graves, J. A. and Podos, J. (2017). Vigor and skill in the acrobatic mating displays of a Neotropical songbird. *Behav. Ecol.* **28**, 164-173.
McHenry, M. J., Claverie, T., Rosario, M. V. and Patek, S. N. (2012). Gearing for speed slows the predatory strike of a mantis shrimp. *J. Exp. Biol.* **215**, 1231-1245.
McHenry, M. J., Anderson, P. S. L., VanWassenbergh, S., Matthews, D. G., Summers, A. P. and Patek, S. N. (2016). The comparative hydrodynamics of rapid rotation by predatory appendages. *J. Exp. Biol.* **219**, 3399-3411.
McNeill, P., Burrows, M. and Hoyle, G. (1972). Fine structure of muscles controlling the strike of the mantis shrimp, *Hemisquilla*. *Zeitschrift für vergleichende Physiologie* **179**, 395-416.
Meijering, E., Dzyubachyk, O. and Smal, I. (2012). Methods for cell and particle tracking. In *Imaging and Spectroscopic Analysis of Living Cells* (ed. P. M. Conn), pp. 183-200. Amsterdam: Elsevier.
Patek, S. N., Korff, W. L. and Caldwell, R. L. (2004). Deadly strike mechanism of a mantis shrimp. *Nature* **428**, 819-820.
Patek, S. N., Nowroozi, B. N., Baio, J. E., Caldwell, R. L. and Summers, A. P. (2007). Linkage mechanics and power amplification of the mantis shrimp's strike. *J. Exp. Biol.* **210**, 3677-3688.
Patek, S. N., Rosario, M. V. and Taylor, J. R. A. (2013). Comparative spring mechanics in mantis shrimp. *J. Exp. Biol.* **216**, 1317-1329.
Payne, R. J. H. (1988). Gradually escalating fights and displays: the cumulative assessment model. *Anim. Behav.* **56**, 651-662.
Pyke, G. H. (1984). Optimal foraging theory: a critical review. *Ann. Rev. Ecol. Syst.* **15**, 523-575.
Reichert, S. E. (1988). The energetic costs of fighting. *Am. Zool.* **28**, 877-884.
Rosario, M. V. and Patek, S. N. (2015). Multilevel analysis of elastic morphology: the mantis shrimp's spring. *J. Morphol.* **276**, 1123-1135.
Rosario, M. V., Sutton, G. P., Patek, S. N. and Sawicki, G. S. (2016). Muscle-spring dynamics in time-limited, elastic movements. *Proc. R. Soc. B* **283**, 20161561.
Schindelin, J., Arganda-Carreras, I., Frise, E., Kaynig, V., Longair, M., Pietzsch, T., Preibisch, S., Rueden, C., Saalfeld, S., Schmid, B. et al. (2012). Fiji: an open-source platform for biological-image analysis. *Nat. Methods* **9**, 676-682.
Schuppe, E. R. and Fuxjager, M. J. (2018). High-speed displays encoding motor skill trigger elevated territorial aggression in downy woodpeckers. *Funct. Ecol.* **32**, 450-460.
Searcy, W. A. and Nowicki, S. (2005). *The Evolution of Animal Communication: Reliability and Deception in Signaling Systems*. Princeton: Princeton University Press.
Számadó, S. (2011). The cost of honesty and the fallacy of the handicap principle. *Anim. Behav.* **81**, 3-10.
Taylor, J. R. A. and Patek, S. N. (2010). Ritualized fighting and biological armor: the impact mechanics of the mantis shrimp's telson. *J. Exp. Biol.* **213**, 3496-3504.
Utter, J. M. and LeFebvre, E. A. (1973). Daily energy expenditure of purple martins (*Progne subis*) during the breeding season: estimates using D_2O^{18} and time budget methods. *Ecology* **54**, 597-604.
Vehrencamp, S. L., Bradbury, J. W. and Gibson, R. M. (1989). The energetic cost of display in male sage grouse. *Anim. Behav.* **38**, 885-896.
Weathers, W. W. and Nagy, K. A. (1980). Simultaneous doubly labeled water ($^3HH^{18}O$) and time-budget estimates of daily energy expenditure in *Phainopepla nitens*. *The Auk* **97**, 861-867.
Wilson, R. S., Angilletta, M. J., James, R. S., Navas, C. and Seebacher, F. (2007). Dishonest signals of strength in male slender crayfish (*Cherax dispar*) during agonistic encounters. *Am. Nat.* **170**, 284-291.
Zack, T. I., Claverie, T. and Patek, S. N. (2009). Elastic energy storage in the mantis shrimp's fast predatory strike. *J. Exp. Biol.* **212**, 4002-4009.